Proceedings of the 20th International Conference on Soil Mechanics and Geotechnical Engineering– Rahman and Jaksa (Eds)

Three-dimensional finite element analysis of a pipe box tunnel in sedimentary rock

Analyse par éléments finis tridimensionnelle d'un tunnel tubulaire dans la roche sédimentaire

Eric Woon & I. Tse
Golder Associates, Australia

S.C. Teo & T.G. Ng
Golder Associates, Singapore

ABSTRACT: Pipe box tunnel (PBT) is a trenchless construction technique trending in a situation where the conventional open-cut-and-cover method is not feasible, due to the presence of critical above-ground structures or the necessity to maintain the functionality of the main roads. Two-dimensional finite element method is commonly adopted in design and analysis of PBT, however, the influence zone of ground deformation around the PBT cannot be reasonably estimated under a plain-strain condition. Limited studies are available on the influence zone during excavation within a pipe box tunnel. The objective of this study is to explore the induced influence zone during the excavation of a PBT adopting a three-dimensional finite element method. A published case study in Singapore, Sentosa Gateway PBT, was back analysed and discussed. The study provides an in-depth understanding on modelling PBT in a three-dimensional finite element, the performance of steel pipes and the deformation of ground during the excavation of PBT. The calculated ground surface settlement for Sentosa Gateway PBT is also compared with settlements measured in a conventional sprayed concrete lining (SCL) tunnels and a circular bored tunnels available in the literature.

RÉSUMÉ : Le tunnel de la boîte à tuyaux (PBT) est une technique de construction sans tranchée tendance dans une situation où la méthode conventionnelle de coupe et de couverture à ciel ouvert n'est pas faisable, en raison de la présence de structures hors sol critiques ou de la nécessité de maintenir la fonctionnalité du principal. routes. La méthode des éléments finis bidimensionnels est couramment adoptée dans la conception et l'analyse du PBT, cependant, la zone d'influence de la déformation du sol autour du PBT ne peut être raisonnablement estimée dans des conditions de déformation simple. Des études limitées sont disponibles sur la zone d'influence lors de l'excavation dans un tunnel tubulaire. L'objectif de cette étude est d'explorer la zone d'influence induite lors de l'excavation d'un PBT en adoptant une méthode des éléments finis tridimensionnels. Une étude de cas publiée à Singapour, Sentosa Gateway PBT, a été analysée et discutée. L'étude fournit une compréhension approfondie de la modélisation du PBT dans un élément fini tridimensionnel, de la performance des tuyaux en acier et de la déformation du sol lors de l'excavation du PBT.

KEYWORDS: Trenchless construction, pipe box tunnel, pipe roof method, three-dimensional finite element, influence zone

1 INTRODUCTION

Road tunnels and underground tunnels are often proposed in a metropolitan area, conventionally constructed using open-cut trench method or cut and cover method. However, conventional methods may not be feasible at times, such as the proposed tunnel is located below existing structures or traffic that cannot be relocated or diverted. Alternative trenchless methods such as the pipe box tunnel method may be feasible.

Pipe box tunnel (PBT) method consists of a series of interconnected hollow steel pipes, forming an enclosed rectangular box-like structure or a pipe box. Once the pipe box is constructed, excavation can be carried within the constructed pipe box tunnel, having minimal disruption to the existing structures or traffic. Several case studies on pipe box tunnel have been published worldwide (Bito 1987; Coller & Abbott 1994; Ahuja & Sterling 2008; Yogarajah et al. 1994; Teo et al. 2016; Ng et al. 2016; Ng et al. 2017).

The most frequent modelling used for PBT is the two-dimensional finite element method (2D FEM). However, due to the plain-strain condition assumed in a two-dimensional finite element analysis, the influence zone of ground deformation around the PBT cannot be reasonably estimated. The influence zone due to the excavation of PBT varies longitudinally and transversely. Limited studies are available on the influence zone during excavation within a pipe box tunnel. This study aims to adopt a three-dimensional finite element method (3D FEM) to back-analyse a constructed PBT, Sentosa Gateway PBT in Singapore, and explore the induced influence zone during excavation of a PBT.

2 SENTOSA GATEWAY PIPE BOX TUNNEL

2.1 *Project description*

Sentosa Gateway Pipe Box Tunnel is a 96 m long vehicular tunnel, connecting outbound traffic from Sentosa Island to mainland Singapore as shown in Figure 1. The tunnel bypasses the busy traffic junctions at Sentosa Gateway, Telok Blangah Road and Kampong Bahru Road. Conventional cut-and-cover method is not feasible due to the presence of Mass Rapid Transit tunnels beneath the proposed road and a network of above-ground roads with high traffic volume.

The proposed PBT is 14.5 m wide by 9.1 m high, located approximately 4 m beneath an existing road with close proximity to several critical structures and utilities. The Mass Rapid Transit tunnels are located about 2 m below the PBT. There are existing viaducts on piled foundation at about 10 m away, where the nearest pile is less than 2 m away from the PBT. More details of the project can be found in Ng et al. (2017).

2.2 *General geology and subsurface condition*

The ground condition of the site generally consists of a sandy silt fill layer of approximately 3 m thick, overlying on residual soils with SPT-N value of 12 increasing with depth to N>100 to the top of sedimentary Jurong Formation at about 10 m to 20 m below ground level. The Jurong Formation comprises of sandstone and siltstone of varying weathering grade. Traces of Kallang Formation consists of unconsolidated estuarine clay, and fluvial soils are encountered at one end of the tunnel. The groundwater table is generally near the ground surface.

Figure 1. Sentosa Gateway Pipe Box Tunnel (PBT) location plan.

2.3 *Construction sequence*

PBT requires a temporary shaft constructed at both ends of the tunnel to install hollow steel pipes (i.e., 813 mm diameter 16 mm thick). A series of steel pipes are installed with a micro tunnel boring machine forming a rectangular pipe box, as shown in Figure 2. After the installation of all the steel pipes, excavation is carried out in stages. At each stage, the excavation is advanced in a 3.5 m interval, where a batter of about 3(V):1(H) with a 1 m wide bench is excavated at the heading, and the exposed batter face is protected with a 100 mm thick shotcrete temporarily until the next excavation stage. A steel frame comprised of steel H-beams (i.e., UB 914x305x313 kg/m) is installed at the toe of the batter before excavation is commenced in the next excavation stage.

For Sentosa Gateway PBT, excavation commences concurrently from both ends of the tunnel. The excavation completes once both excavation front meets at the middle of the tunnel. The construction of the permanent road structure commences upon completion of excavation.

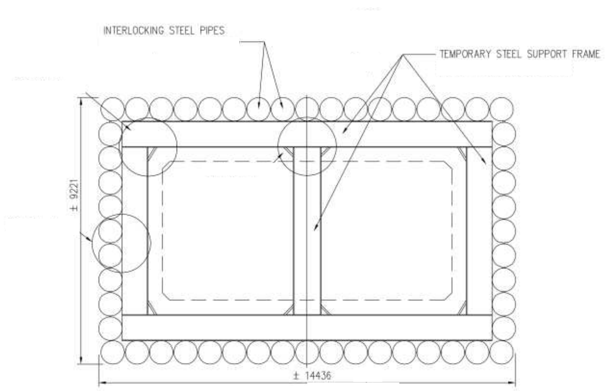

Figure 2. Cross-section of PBT (Teo et al. 2016).

2.4 *Monitoring of PBT*

The vertical displacement of the pipe roof is monitored by a series of prisms placed within a top steel pipe, middle of the PBT, spaced at 10 m apart along the steel pipe. The displacement of the steel pipe was monitored during the excavation of PBT.

3 THREE-DIMENSIONAL FINITE ELEMENT ANALYSIS

PLAXIS 3D finite element analysis software, a tool widely applied in the field of engineering, will be the approach used for the tunnel excavation in a PBT. Due to the relatively long tunnel relative to the depth, in this present study, the excavation from both ends of PBT was modelled in two separate models, with both models ends at the alignment mid-point, as shown in Figure 3.

Because of the symmetry condition of the PBT, only half of the PBT along the tunnel-centreline was modelled. The model is sufficiently large to avoid boundary effects with 5D (D=equivalent tunnel diameter of 9 m) in the transverse direction to the PBT and 1D to the bottom boundary. Note that the PBT is underlain by competent rock (i.e., SIII) where negligible deformation is expected. Sensitivity analyses confirmed these assumptions by varying model size. Boundary conditions were defined as follows: the ground surface is free to displace, the normal directions are fixed in the vertical boundaries and the base of the model. The steel pipe is 'detached' from the side boundary condition to simulate the simply-supported connection where the steel pipe is able to rotate freely. The steel pipe is 'detached' by modelling a sufficiently soft linear elastic element between the steel pipe and the side boundaries. The mesh in the vicinity of the tunnel excavation was densified as these zones have great relevance for deformation results.

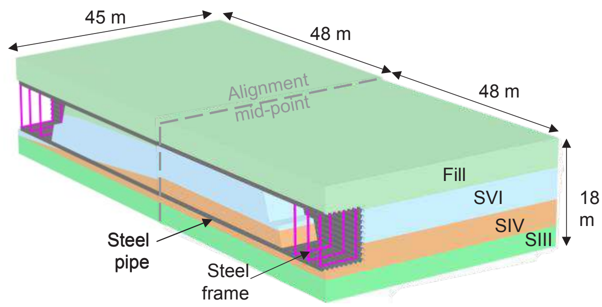

Figure 3. Three-dimensional finite element model

The hardening soil model was used in the finite element analysis and adopted the same Mohr-Coulomb failure criterion parameters as presented in Teo et al. (2016). The hardening soil model can simulate stress-dependent stiffness, which best predicts soil deformation behaviour. Modelling of the steel pipe was performed using solid extrusion elements, in an octagon shape with a linear elastic model. The Young's modulus of the linear elastic solid octagon is back-calculated from the flexural stiffness of the hollow steel pipe (i.e., 813 mm diameter 16 mm thick). A separate prototype model of PBT, a simply supported PBT over a span of 10 m, was modelled to validate the settlement of a solid octagon is comparable to a hollow pipe as shown in Figure 4.

The staged excavations of PBT are simulated through the following analysis steps:

- Generation of in-situ stress.
- Installation of steel pipes and steel frame at the entrance.
- Excavation of 3.5 m of soil forming a batter of about 3(V):1(H) with a 1 m wide bench and subsequent installation of steel frame at 3.5 m from the toe of the batter. This step is repeated to simulate the subsequent excavation stage.

The analysis steps simulate the excavation starting from one end of the model towards the other end, the alignment mid-point, as shown in Figure 3.

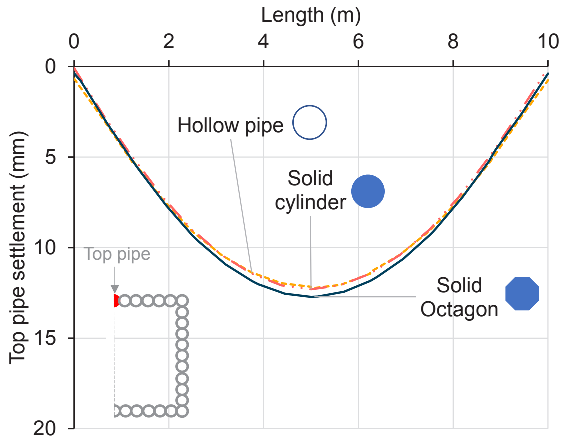

Figure 4. Computed settlement of simply supported model pipes.

4 RESULTS AND DISCUSSION

4.1 *Comparison between computed and measured results*

Figure 5 shows the maximum top of pipe settlement computed in 3D FEM at the end of the excavation. The computed and measured top pipe settlement as published in Teo et al. (2016) is also included in the figure for comparison. The maximum computed top pipe settlement by 3D FEM is comparable to the measured settlement. Note that the results from 3D FEM as shown in the figure are computed from two 3D FEM models as described in the previous section. Due to the presence of Kallang formation towards the west of the PBT (i.e., 0 m to -50 m), the computed top pipe settlement at the mid-point of the alignment (i.e., Distance from alignment mid-point = 0 m) varies between the two models. The top pipe settlement estimated by 3D FEM lies between the measured settlement and computed settlement by 2D FEM.

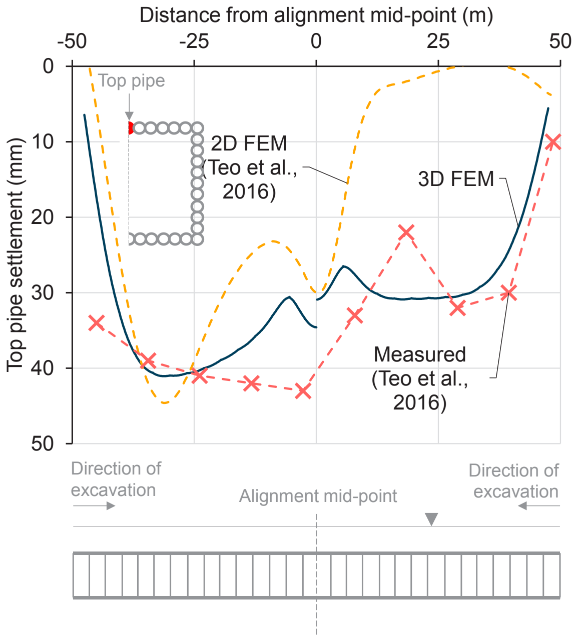

Figure 5. Computed and measured top steel pipe settlements at the completion of excavation.

Figure 6 compares the computed (in 3D FEM) and measured top pipe settlement at the selected excavation stage as depicted by a schematic diagram below at each figure. The computed top pipe settlement match reasonably well with the measured top pipe settlement at each stage. In comparison with the settlement computed in the final excavation stage (i.e., Figure 5), the variation between the computed and measured settlement is observed to be larger in the final excavation stage. The larger settlement that was computed may be due to the assumed boundary condition along the alignment mid-point in each of the 3D FEM models, becoming more apparent when the excavation stage progresses towards the alignment mid-point/the model boundary.

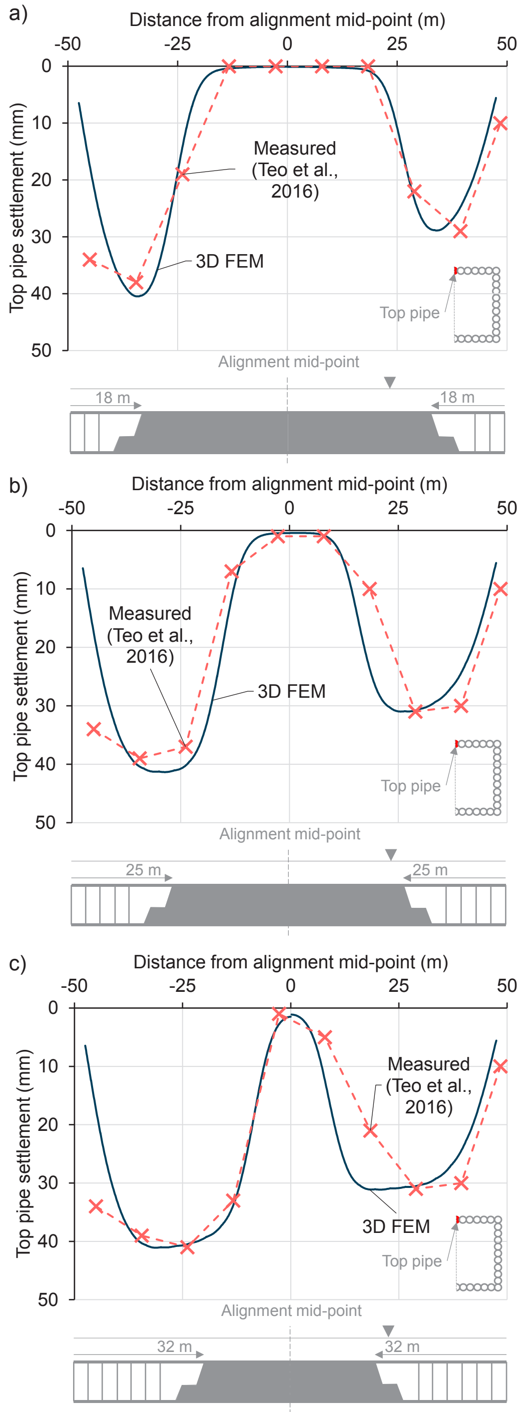

Figure 6. Computed and measured top steel pipe settlements when excavation face at: (a) 18 m, (b) 25 m and (c) 32 m.

4.2 *Influence zone induced by excavation in PBT*

Figure 7 shows the displacements of steel pipe located at the top, side and bottom of the PBT when excavation face progress to 25 m. During excavation within the PBT, the PBT undergoes stress relief, resulting in all the steel pipes displaced towards the excavated side. Higher displacement is computed in the top pipe as compared to the side and bottom pipe. The higher displacement that was computed may be due to the ground being stiffer with increasing depth, and higher stiffness is adopted for unloading compared to loading in the hardening soil model.

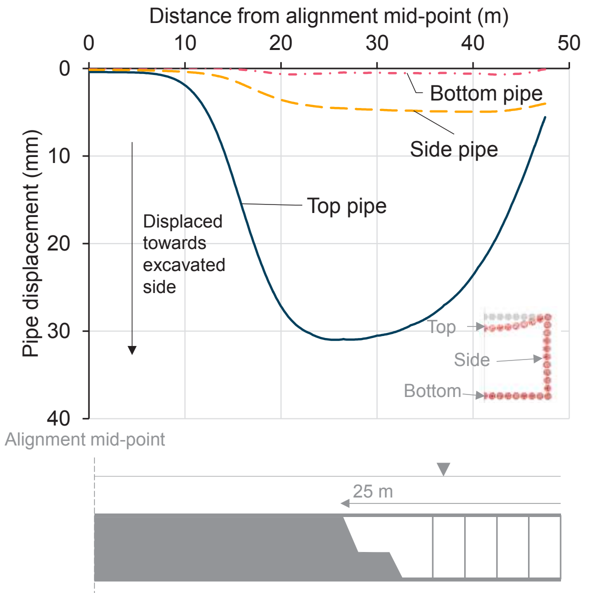

Figure 7. Computed displacement of steel pipes.

Figure 8 shows the computed displacement contour at excavation stage of 25 m. Higher ground displacement is observed at the top of PBT, observed to be dependent with the settlement of the top pipe. As shown in Figure 9, the extent of ground surface settlement is identical to the settlement of the steel pipe. Due to soil arching, the magnitude of ground surface settlement is lesser than the settlement of the top pipe.

Generally, the steel pipe is supported by steel frames and the retained ground in the PBT at each excavation stage. During excavation, the steel pipe settles within the lengths of unsupported 'excavated' and the 'retained' as demarcated in Figure 8 and Figure 9(a), but not within the 'supported' length. Once the steel frame is installed, negligible pipe settlement is expected within this 'supported' length when the excavation progresses for the remaining stages.

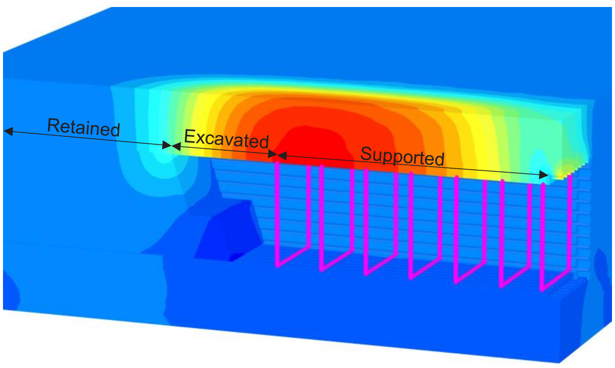

Figure 8. Computed displacement colour contour plot.

At each excavation stage, the induced influence zone in the longitudinal direction is observed to be extending about 20 m (i.e., 2D) ahead from the excavation face as shown in Figure 9(a). In the transverse direction, most of the ground settlement is observed to be induced directly above the PBT as excavation progresses. The influence zone may extend to about 10 to 25 m (i.e., 1D to 2.5D) from the tunnel centerline.

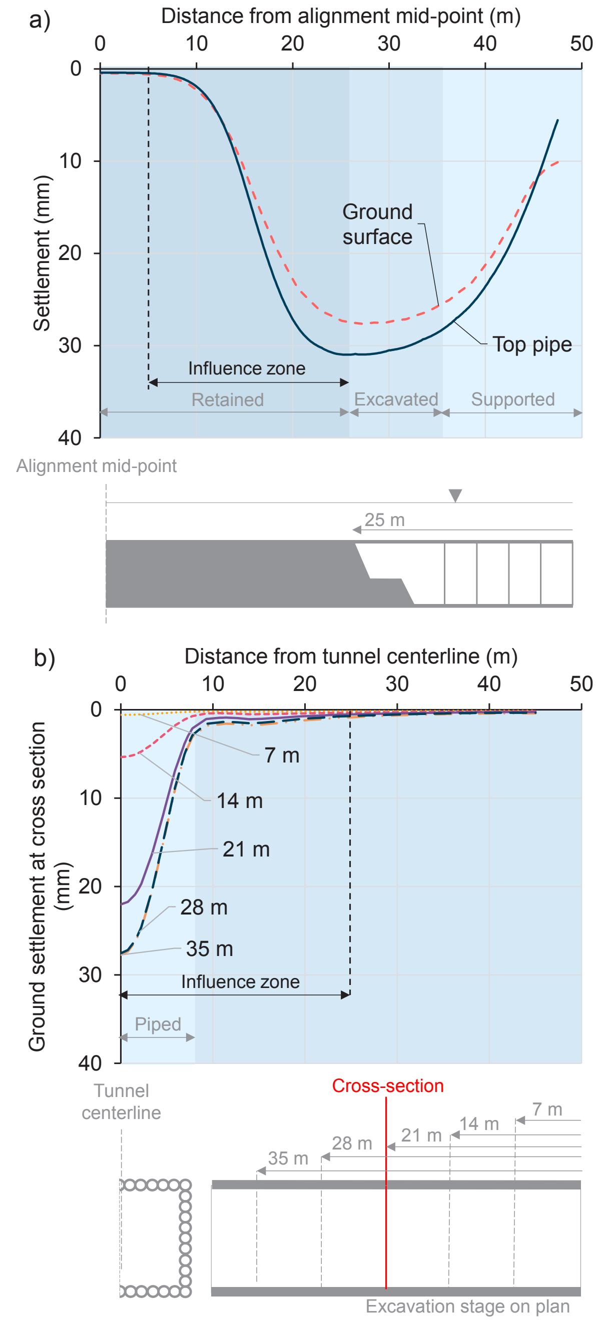

Figure 9. Induced influence zone in the: (a) longitudinal and (b) transverse direction.

4.3 *Comparison with other published shallow tunnels*

Figure 10 compares a maximum settlement (s) at ground surface for PBTs (Moh et al., 1999), sprayed concrete lining (SCL) tunnels reinforced with pipe canopy (Sigl, 2020) and circular bored tunnels (Chou & Bobet, 2002) that are available in the literatures. The maximum ground surface settlement is normalised with the diameter of tunnel (s/D). For the diameter of a PBT, an equivalent diameter is calculated from the cross-sectional area of a PBT. The normalised ground surface settlements (s/D) are presented to the respective cover-to-diameter ratio (C/D) of each tunnel.

The C/D for circular bored tunnels are generally more than one as compared to PBTs, including the Sentosa Gateway PBT, where the C/D is generally less than 0.5. The normalised ground surface settlement measured in PBT is generally lower than those in SCL tunnels or circular bored tunnels.

The normalised ground surface settlement for various C/D estimated based on the method proposed by Peck (1969), is also included at various volume loss (V) expressed at a percentage of the cross-sectional tunnel excavated area. The calculated normalised settlements assumed a parameter K of 0.45. The estimated volume loss for PBT is expected to be less than 0.5%, as compared to the volume loss for SCL tunnels or bored circular tunnels of about or more than 1%.

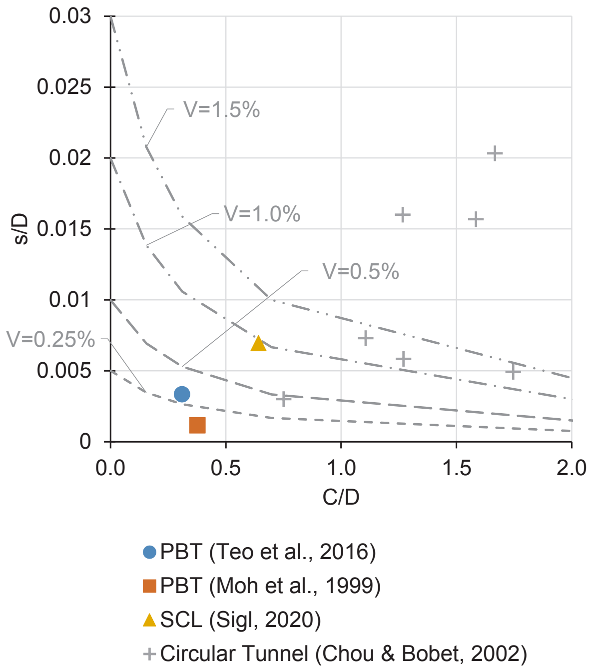

Figure 10. Measured surface settlements in PBT and circular tunnels

5 CONCLUSIONS

The design and analysis of a PBT is commonly carried out using a 2D FEM. This study takes advantage of a 3D FEM which can compute the displacement in both longitudinal and transverse direction to investigate the induced influence zone during the excavation of the PBT. The main findings of this study include:

- Due to the scales difference in a PBT, where the length of a PBT can be in the order of 100 m and the diameter of a steel pipe is about 1 m, it may be challenging to mesh in a 3D FEM. Given the symmetrical geometric condition of the Sentosa Gateway PBT, a half model along the tunnel centerline is modelled. As the excavation progresses from both ends of the PBT symmetrically, the half model is analysed in two separate models separated along the alignment mid-point.
- Meshing issues may arise when modelling circular pipes supported by steel frames. The modelling of a circular hollow pipe can be replaced with a solid octagon pipe.
- The steel pipes in a PBT are supported by steel frames and retained soil in a PBT at each excavation stage. The steel pipes displaced towards the excavated side during excavation, where the highest displacement is observed at the top row of pipes, middle of the PBT. The excavation of PBT is analogous to squeezing a toothpaste tube. The placing steel frames within a PBT is analogous to placing a surgical stent in a blood vessel to maintain the blood flow.
- The computed ground surface settlement is similar to the computed top pipe settlement induced by excavation. The induced influence zone extends to about 2D ahead of the excavation face and 1D to 2.5D from the tunnel centerline.
- The ground settlement published for a PBT is generally less than conventional SCL tunnels or circular bored tunnels, with volume loss expected not more than 0.5%.

6 REFERENCES

Ahuja, V. and Sterling, R.L., 2008. Numerical modelling approach for microtunnelling assisted pipe-roof support system. In *World Tunnel Congress* (pp. 1678-1687).

Bito, Y., 1987. Construction methods of the structures passing through under railway lines. *Japanese railway engineering*, (101), pp.6-9.

Chou, W.I. and Bobet, A., 2002. Predictions of ground deformations in shallow tunnels in clay. Tunnelling and underground space technology, 17(1), pp.3-19.

Coller, P.J. and Abbott, D.G., 1994. Microtunneling techniques to form an insitu barrier around existing structures. In *High Level Radioactive Waste Management: Proceedings of the fifth annual international conference. Volume 2*.

Moh, Z.C., Hsiung, K.I., Huang, P.C. and Hwang, R.N., 1999, November. Underpass beneath Taipei international airport. In Proc. Conference on New Frontiers and Challenges.

Ng, T.G., Yogarajah, I., Teo, S.C. and Pan, H.Y., 2017. Trenchless construction of Sentosa Gateway Tunnel. In *16th Australasian Tunnelling Conference 2017: Challenging Underground Space: Bigger, Better, More* (p. 552). Engineers Australia.

Ng, T.G., Yogarajah, I., Woon, K.X., Teo, S.C. and Adalarasu, J., 2016, May. Trenchless Construction of Underground Infrastructures in Singapore. In *Proceedings of the 19th Southeast Asian Geotechnical Conference & 2nd AGSSEA Conference Malaysia 2016* (pp. 149-155).

Peck, R.B., 1969. Deep excavations and tunneling in soft ground. Proc. *7th Int. Conf. on Soil Mechanics and Foundation Engineering*, pp.225-290.

Sigl, O., 2020. Special construction methods for tunnels with very shallow overburden–Challenge for innovation. Geomechanics and Tunnelling, 13(6), pp.634-640.

Teo, S.C., Ng, T.G., Yogarajah, I., Woon, K.X. and Dang, H.P., 2016, December. Two-Lane vehicle underpass using pipe roof method at Sentosa Gateway Tunnel. In *Challenges and Innovations in Geotechnics: Proceedings of the 8th Asian Young Geotechnical Engineers Conference, Astana, Kazakhstan, August 5-7, 2016* (p. 105). CRC Press.

Yogarajah, I., Chua, T.S. and Ganeshan, V., 1994. Microtunnelling for Underpass Construction in Built-Up Areas. In *2nd National Trenchless Technology Conference*.